Metastable 9-fluorenone: Blue-shifted fluorescence, single-crystal-to-single-crystal reactivity, and evaluation as a multi-modal fingermark visualization treatment

Grace E. Florence,[a] Katy A. Bruce,[a] Helena J. Shepherd,[a] and William J. Gee*[a]

Dedication ((optional))

Abstract: A metastable form of 9-fluorenone (MS9F) has been characterized using Raman spectroscopy, fluorimetry, and X-ray diffraction techniques. MS9F emits blue fluorescence (λ_{max} = 495 nm) upon 365 nm irradiation and undergoes a single-crystal-to-single-crystal (SCSC) transformation to reach the ground state form (GS9F) over ca 30 minutes, whereupon it emits the expected green fluorescence. A structure-property relationship for this fluorescent behavior has been posited. MS9F and GS9F were applied as a means of visualizing latent fingermarks on a non-porous surface. This approach identified three different modes of fluorescent fingermark visualization using 9-fluorenone.

Latent fingerprints (i.e. fingermarks) constitute important forensic evidence. Fingermark residues contain an emulsion of polar (e.g. amino acids) and nonpolar (e.g. lipids) dermal components. Of these, the nonpolar fraction is more resistant to environmental degradation, and thus persists longer on surfaces than the polar fraction.[1] For this reason, new visualization methods that target the nonpolar components of fingermarks provide great interest to the forensic community. Our previous work has shown that sublimation can be harnessed to direct luminescent chemical reagents, e.g. lanthanide complexes, into the lipid fraction of fingermarks to aid visualization.[2] This work aims to complement the established fingermark visualization technique vacuum metal deposition (VMD), which is known for its high sensitivity and applicability across a wide range of surfaces.[3] VMD could be improved by developing inherently luminescent fingermark coatings, as presently this is achieved by applying additional treatments, such as fluorescent staining with Basic Yellow 40.[4] Additional steps such as this complicate and lengthen the VMD process, and risk damaging the fragile fingermark evidence.

While effective, the luminescent rare earth method to visualize fingermarks is not as cost-effective as other strategies.[1,2] By comparison, many small organic fluorophores are inexpensive, and offer a wide diversity of emission profiles spanning the visible spectrum. 9-Fluorenone is one such small organic fluorophore, and it forms the basis of many luminescent molecular devices and materials. This is exemplified by fluorenone scaffolds found in light emitting diodes,[5] charge-transfer compounds,[6] copolymers,[7] devices for studying protein-ligand interactions,[8] and organic solar cells.[9] 9-Fluorenone has enabled fundamental study of fluorescent processes such as quenching,[10] population of excited states,[11] two-photon absorption processes,[12] and theoretical modelling studies in both the gas– and solution–phase.[13] Given the importance of the 9-fluorenone motif to emissive materials,[14] this discovery of a new polymorph provides new insights from a proposed structure-property relationship, potentially guiding the design of new materials.

The fluorescent behavior of the archetypal species, 9-fluorenone, has been extensively studied in solution.[15] In this medium the fluorescent emission is highly susceptible to perturbation by both solvent polarity and temperature.[13,15] This is exemplified by shifting of the emission maximum from ca 500 nm for the nonpolar aprotic hexane, to 570 nm in the polar protic solvent methanol owing to the influence of hydrogen bonding.[13] This wavelength range is ideal for forensic applications because it spans the optimal detection range of the human eye.[16] The physical properties of 9-fluorenone are similarly interesting, with a sublimation vapor pressure of 0.0121 Pa and an enthalpy of sublimation of 88.5±3.7 kJ mol^{-1} at 300 K,[17] and suggest that sublimation represents a viable vector of delivery into a latent fingerprint.

Given the well-documented physical properties of 9-fluorenone, and an established protocol for delivery of volatile species into fingermark residues,[2] work began by applying fluorenone using this prior protocol. Uptake of 9-fluorenone into the fingermark was apparent even without optimizing the heating and vacuum conditions (Fig. 1, Details of the fingermark study and subsequent visualization conditions listed in ESI). Unexpectedly, two distinct luminescent species were clearly visible. These correspond to the expected green-emitting ground-state 9-fluorenone (GS9F), and a previously unreported metastable blue-emitting form (MS9F). Past characterization of solid-state 9-fluorenone has been limited to a poorly-resolved absorption spectrum with a maximum at ca λ = 395 nm, and an emission maximum at λ = 510 nm.[18] To the best of our knowledge, no metastable forms of 9-fluorenone have been reported to date. Given the ubiquity of 9-fluorenone and its derivatives in fluorescent materials, coupled with the promise of forensic science

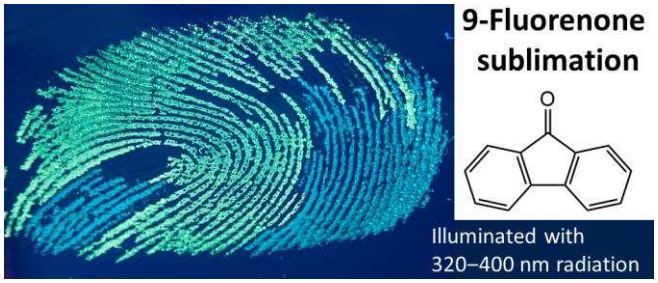

Figure 1. The unexpected observation of two luminescent 9-fluorenone species after unoptimized chemical treatment of a latent fingermark. GS9F emits green fluorescence, whereas MS9F produces a blue-shifted emission.

[a] Miss G. E. Florence, Mrs K. A. Bruce, Dr H. J. Shepherd and Dr W. J. Gee
School of Physical Sciences
University of Kent
Canterbury, Kent, CT2 7NH (UK)
E-mail: W.Gee@kent.ac.uk

Supporting information and the ORCID identification number(s) for this article is given via a link at the end of the document.

applications, the new metastable form identified in this work offers important insights. A structure-property relationship rationalizing the differences in emission properties is proposed below, and a study exploring delivery of either GS9F, or MS9F, into fingermark residues is reported. The differences in emission spectra between the two polymorphs enables the possibility of multi-modal visualization of fingermarks using a specific desired fluorescent form.

Large quantities of metastable MS9F were sourced during this study by dropping molten 9-fluorenone onto aluminum foil whereupon rapid crystallization occurs. Screening the resultant MS9F and GS9F forms was performed using a UV light source (λ = 365 nm) and manually sorting the products according to color of the fluorescent emission, with approximately half the material typically adopting the metastable form. Bulk purity of MS9F was confirmed using powder X-ray crystallography (ESI, Fig. S2), with the measured diffraction pattern matching the features predicted from single crystal measurements performed on the metastable species. Analysis of both species by thermogravimetric analysis showed that MS9F has a depressed melting point onset of 72.8 ℃ relative to GS9F at 84.4 ℃. Continued heating resulted in slow onset of mass loss for both species from ca 100 °C as 9-fluorenone volatilizes (ESI, Fig. S3, S4).

Solid-state fluorimetry was used to characterize and compare the excitation and emission characteristics of MS9F and GS9F. The ground state form, GS9F (Fig. 2, green trace), has a broad emission profile spanning 450–700 nm when irradiated at 365 nm. The maxima is located at 515 nm, corresponding to the expected green color. These emission characteristics are blue-shifted for MS9F (Fig. 2, blue trace), with an emission maximum located at 495 nm, and an emission profile spanning from 430–650 nm.

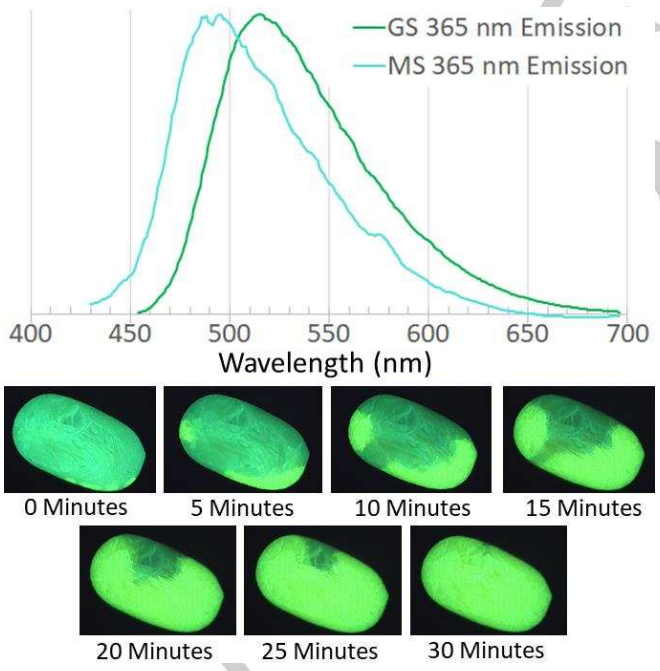

Figure 2. Top: A comparison of the emission profile for both MS9F (blue trace) and GS9F (green trace) when irradiated at 365 nm in the solid-state. Bottom: The SCSC transformation of MS9F to GS9F occurring over 30 minutes with an image taken every 5 minutes.

Single crystals of MS9F that were suitable for X-ray diffraction studies were grown by slow-cooling of 9-fluorenone dissolved in hot mineral oil. Full details of synthetic procedures and an expanded crystallographic discussion are available as ESI. The diffraction pattern of MS9F contains first-order satellite peaks corresponding to an incommensurate modulation of the crystal structure, as described in more detail in the supplementary information. Full analysis of the incommensurate modulation is beyond the scope of the present communication and consequently the structure was refined only against the main Bragg reflections. The result is a model displaying whole molecule disorder, with two possible orientations of the molecule that are approximately coplanar, related by an inversion center, each with 50% occupancy. While it is possible to compare overall crystal packing motifs between MS9F and GS9F it is important to note that no conclusions as to the long-range order of specific intermolecular interactions can be drawn from this model.

In order to compare the differences in structure and resultant fluorescent properties it is necessary to briefly revisit the known GS9F structure.[21] The asymmetric unit of GS9F contains two crystallographically distinct molecules, which form a dimer through π-π stacking interactions, as shown in the green box in Figure 3, with interplanar distances between the rings between 3.50 and 3.65 Å. The molecules are oriented such that the keto groups are aligned parallel. There are no further significant supramolecular interactions between adjacent molecules in GS9F. By contrast, in MS9F, it is possible for molecules to be oriented such that their keto groups are aligned antiparallel, as shown in the blue box in Figure 3. Intermolecular ketone distances of 3.088(X) Å for C(1)···O(1') and O(1)···C(1') imply the formation of bond dipole-dipole interactions occurring between adjacent opposing keto groups. This difference in ketone environment may well be responsible for the observed differences in the emission spectra of the two compounds.

The ability of dipole-dipole interactions to direct crystal structure has been debated,[19] however functional groups with strong dipole moments, such as nitriles (3.6 D) or ketones (2.9 D), are known to influence the orientation of neighboring molecules when in close proximity (<3.6 Å).[20] Despite the planar aromatic nature of 9-fluorenone, no π–π stacking interactions were evident in the metastable MS9F structure. Weak C–H···O hydrogen bonding has been found to meaningfully contribute to stabilization of specific crystal forms under certain conditions,[22] however such interactions do not appear to influence the solid-state structures of either MS9F or GS9F, given that the donor–acceptor distances are >3.4 Å, and owing to non-optimal directionality of the hydrogen donor atoms.

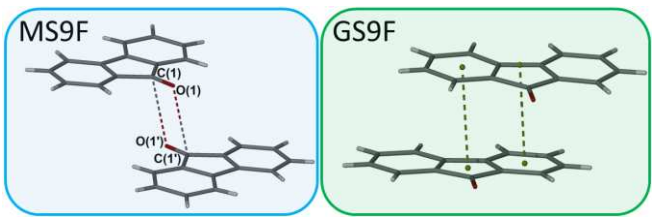

Figure 3. Blue box: The solid-state structure of MS9F. The proposed ordering force, bond dipole-dipole interactions, occurs between antiparallel keto groups. Green box: The solid-state structure of GS9F.[21] Here the dominant ordering force is π–π stacking interactions between aromatic rings of 9-fluorenone.

The proposed link between different ketone environments of MS9F and GS9F, and changes to the fluorescent emission wavelength, is supported by aforementioned theoretical studies.[13] In that study, the magnitude of the C=O dipole correlated with changes to the Stokes shift which, in solution–state studies, was perturbed by varying degrees of hydrogen bonding with different solvent species. Here, we suggest that the same effect is triggered as a result of the presence or absence of bond dipole-dipole interactions within the crystalline lattice. Out-of-plane bending of the C=O group also impacts intersystem crossing within the molecule,[13] influencing the excitation energies of 9-fluorenone and altering the emission color.

Large structural differences are evident when comparing the crystalline lattice arrangements of MS9F and GS9F. Consequently, the observation that the metastable-form undergoes conversion to the ground-state form in a single-crystal-to-single-crystal transformation is noteworthy. This transformation occurs slowly (ca 30 minutes, Fig. 2, bottom) by propagation through the crystal in a cascading fashion from a point of initiation, reminiscent of 'molecular domino transformations' reported for certain metal complexes.[23] Significant rotation of molecules is required for this solid-state transformation, and similar scale single-crystal-to-single-crystal transformations have been previously reported,[24] including those in which discrete molecular species rotate as much as 180° within a crystalline lattice.[25]

Understanding of this dynamic process allowed optimization of selective delivery of each form into fingermark residues. Fingermarks were placed on aluminum foil and small quantities of 9-fluorenone (20 mg) were transferred into a vial, followed by a plug of cotton wool. The aluminum foil bearing the fingermark was then placed above the plug, and the vial was sealed with a crimp cap and placed under vacuum (4.0×10^{-1} mbar). The sealed vial was then transferred to an oven and subjected to varying temperature and time durations. The resulting visually-determined ratios of MS9F to GS9F are shown in Table 1 (selected images provided in ESI).

The results in Table 1 show a general trend in which MS9F preferentially forms at lower temperatures (<140 ℃) and in shorter duration experiments. This suggests that formation of MS9F is favorable upon delivering lower concentrations of 9-fluorenone into fingermark residues, however the extended cooling time needed for the higher temperature experiments may also contribute to the greater prevalence of GS9F. At higher temperatures (>160 ℃) degradation of the fingermark becomes a significant problem, which appears to be the result of excessive deposition of 9-fluorenone into the fingermark residues, causing ridges to expand and fuse together, obscuring the overall pattern.

The optimal treatments to target specific 9-fluorenone forms were found to be 60 minutes at 130 ℃ for MS9F, and 90 minutes at 160 ℃ for GS9F. Treating fingermarks in either way was found to produce third level ridge details, i.e. pore locations within the ridge patterns (Fig. 4, center and right). Interestingly, viewing the treated fingermarks directly after removal from the oven resulted in a third means of visualizing the prints, wherein crystallization of either form had yet to take place. This non-crystalline form (Fig. 4, left) is less emissive relative to the two crystalline forms, requiring more intense UV radiation to deliver similar contrast. This finding suggests that the viscosity change is a key mechanism that promotes luminescent emission from 9-fluorenone.[26] Full fingermark images of MS9F and GS9F treated fingermarks are shown in the ESI (Fig. S8).

Figure 4. The three modes of visualization provided by the 9-fluorenone treatment. Left: non-crystalline or amorphous 9-fluorenone. Centre: metastable MS9F. Right: ground state GS9F. The pore locations within the fingermark ridges are evident in each image. Images were visualized using a LUMATEC Superlite S04 forensic light source emitting 320–400 nm radiation and photographed with a Nikon D300 camera coupled with a DX Micro NIKKOR 40 mm Lens without filters.

Raman spectroscopy was used to confirm that the two forms of 9-fluorenone present in the fingermarks were the crystalline samples GS9F and MS9F analyzed in this study. The Raman analysis comprised four spectra: a reference sample of commercial GS9F; a separate reference spectrum of MS9F that was later structurally confirmed as the metastable form by powder X-ray diffraction; and two sample spectra obtained from two separate treated fingermark residues proposed to contain either GS9F or MS9F. The fingermark samples were laid on aluminum foil surfaces to negate surface interference.[27] Full spectra with experimental details are provided in the ESI (Fig. S9-S11). Comparing the spectrum of either GS9F or MS9F present within the fingermark to its corresponding reference

Table 1. Optimization study measuring the uptake of 9-fluorenone by fingermarks placed on aluminum foil at 4.0×10^{-1} mbar. Both temperature and duration of heating were investigated, and the dominant form of 9-fluorenone is listed (MS = metastable; GS = ground state). Where both MS9F and GS9F were observed within the treated fingermark, the %-ratio of each is estimated in the parentheses. Images of selected treated fingermarks are shown in the ESI.

9-Fluorenone

Time (min) \ Temperature (°C)	85	100	110	120	130	140	150	160	180
30					MS	MS	MS (80:20)	GS (80:20)	GS (95:5)
60			MS	MS	MS (100)	MS (95)	MS (60:40)	GS (95:5)	GS (100)
90		MS	MS (70)	MS (100)	MS (100)	GS (85:15)	GS (66:33)	GS (100)	GS (100)
120	MS	MS (65:10)	MS (90:5)	MS (100)	MS (90:10)	GS (100)	GS (100)	GS (100)	GS (100)

No visualisation / degradation
Partial visualisation (<50%)
MS9F dominant
GS9F dominant

spectrum revealed matching features. Similarly, no additional peaks were evident in either fingermark spectrum. This confirms the identity of crystalline GS9F and MS9F as the emissive species present within the fingermarks after treatment. Both fingermark spectra exhibited greater fluorescence and a more undulating baseline than the reference samples, which likely derive from fingermark sebum or other biological residues.[28]

The most significant peak differences in the Raman spectra derived from the fingermark samples containing either GS9F or MS9F corresponded to unique lattice and ketone environments (Fig. 5). There is a peak in the low energy phonon region for GS9F that appears at 85 cm^{-1}, while in MS9F a peak is found at 102 cm^{-1}. This is indicative of a significant change in the long-range translational symmetry between the two crystal structures. The ketone stretching mode shifts from 1712 cm^{-1} for GS9F to 1719 cm^{-1} for MS9F, and can be attributed to a change in chemical environments at the ketone upon transition between the polymorphic forms. Both findings are supported by the observations made in the X-ray diffraction study discussed above.

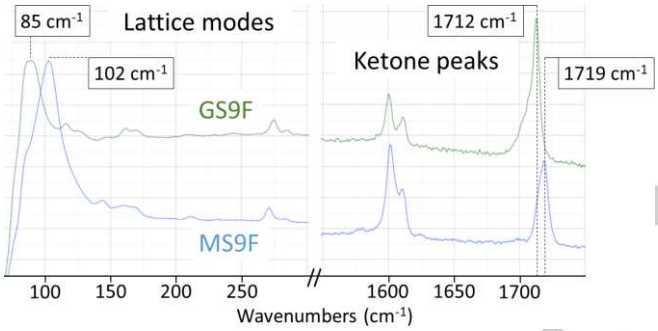

Figure 5. The unique lattice and ketone environments observed for GS9F (green upper trace) and MS9F (blue lower trace) present within fingermark samples placed on aluminum foil when analyzed by Raman spectroscopy.

The sum of these results showcase a new metastable form of 9-fluorenone, its physical properties, and its ability to contribute to the visualization of fingermarks. Single-crystal X-ray diffraction methods provide a structural comparison of the metastable and ground-state forms, enabling a plausible structure-property relationship linking the chemical environment of the keto group within the crystalline lattice to the Stokes shift of the fluorescent emissions. The metastable form was found to convert over the space of 30 minutes to the ground-state form by a single-crystal-to-single-crystal transformation, in which molecules of 9-fluorenone must rotate significantly. Finally, the ability to selectively impart either form into fingermark residues to allow their fluorescent visualization was achieved. This work shows that the metastable form, the ground-state form, and a non-crystalline form could all be infused into fingermarks, each providing a unique fluorescent emissive profile. These preliminary findings show promise for multimodal imaging of fingermarks using a single chemical reagent, however further work is needed to validate this method in a forensic context. Limitations of the current work include that only a single surface type was investigated, that the fingermarks were not aged beyond 24 hours, and that only a relatively small pool of fingermarks / donors were evaluated (See ESI for full study details). A thorough overview of the factors needing consideration when undertaking fingermark research was recently published by the International Fingerprint Research Group.[29] These guidelines provide detailed assessment criteria for evaluating the results of pilot studies such as this.

Acknowledgements

We are grateful to both the Royal Society (RG170176) and the Royal Society of Chemistry (RF18-4963) for financial support of this work.

Conflict of Interest

The authors declare no conflict of interest.

Keywords: Fluorescence • Forensics • Fingermark • Fluorenone • Raman spectroscopy

[1] C. Champod, C. J. Lennard, P. Margot and M. Stoilovic in Fingerprints and Other Ridge Skin Impressions, 2nd ed., CRC Press, Boca Raton, 2016.
[2] G. E. Florence and W. J. Gee, Analyst, **2018**, 143, 3789.
[3] a) P. Theys, Y. Turgis, A. Lepareux, G. Chevet and P. F. Ceccaldi, Rev. Int. Police Crim., **1968**, 23, 106. b) T. Kent, G. L. Thomas, T. E. Reynoldson and H. W. East, J. Forensic Sci. Soc., **1976**, 16, 93.
[4] N. Jones, M. Kelly, M. Stoilovic, C. Lennard and C. Roux, J. Forensic Ident., **2003**, 53, 50.
[5] W. Porzio, S. Destri, M. Pasini, U. Giovanella, M. Ragazzi, G. Scavia, D. Kotowski, G. Zotti and B. Vercelli, New J. Chem., **2010**, 34, 1961.
[6] Y. Li, T. Liu, H. Liu, M.-Z. Tian and Y. Li, Acc. Chem. Res., **2014**, 47, 1186.
[7] L. Romaner, A. Pogantsch, P. Scandiucci de Freitas, U. Scherf, M. Gaal, E. Zojer and E. J. W. List, Adv. Mater., **2003**, 13, 597.
[8] A. K. Feldman, M. L. Steigerwald, X. Guo and C. Nuckolls, Acc. Chem. Res., **2008**, 41, 1731.
[9] a) T.-T. Do, J. Subbiah, S. Manzhos, D. J. Jones, J. M. Bell and P. Sonar, Org. Electron., **2018**, 62, 12. b) T. T. Do, K. Rundel, Q. Gu, E. Gann, S. Manzhos, K. Feron, J. Bell, C. R. McNeill and P. Sonar, New J. Chem., **2017**, 41, 2899. c) T. T. Do, H. D. Pham, S. Manzhos, J. M. Bell and P. Sonar, ACS Appl. Mater. Interfaces, **2017**, 9, 16967.
[10] a) G.-J. Zhao and K.-L. Han, J. Phys. Chem. A, **2007**, 111, 9218. b) L. Biczok, T. Berces and H. Linschitz, J. Am. Chem. Soc., **1997**, 119, 11071.
[11] a) P. J. Homnick, J. S. Tinkham, R. Devaughn and P. M. Lahti, J. Phys. Chem. A, **2014**, 118, 475. b) M. W. D. Hanson-Heine, J. A. Calladine, J. Yang, M. Towrie, R. Horvath, N. A. Besley and M. W. George, Chem. Phys., **2018**, 512, 44.
[12] J. Dipold, R. J. M. B. Batista, R. D. Fonseca, D. L. Silva, G. L. Moura, J. V. dos Anjos, A. M. Simas, L. De Boni and C. R. Mendonca, Chem. Phys. Lett., **2016**, 661, 143.
[13] C.-W. Chang, T. I. Soelling and E. W-G. Diau, Chem. Phys. Lett., **2017**, 686, 218.
[14] a) V. S. Thirunavukkarasu, K. Parthasarathy and C.-H. Cheng, Angew. Chem. Int. Ed., **2008**, 47, 9462. b) M. A. Campo and R. C. Larock, J. Org. Chem., **2002**, 67, 5616. c) G. Yang, Q. Zhang, H. Miao, X. Tong and J. Xu, Org. Lett., **2005**, 7, 263. d) R. Ruzi, M. Zhang, K. Ablajan and C. Zhu, J. Org. Chem., **2017**, 82, 12834. e) L. Liu, J. Qiang, S. Bai, Y. Li, C. Miao and J. Li, Appl. Organomet. Chem., **2017**, 31, e3817.
[15] a) A. Kuboyama, Bull. Chem. Soc. Jpn., **1964**, 37, 1540. b) T. Kobayashi and S. Nagakura, Chem. Phys. Lett., **1976**, 43, 429. c) L. J.

Andrews, A. Deroulede and H. Linschitz, J. Phys. Chem., **1978**, 82, 2304. d) L. Biczók and T. Bérces, J. Phys. Chem., **1988**, 92, 3842.
[16] J. J. Vos, Colour Research & Application, **1978**, 3, 125.
[17] J. L. Goldfarb and E. M. Suuberg, J. Chem. Thermodyn., **2010**, 42, 781.
[18] K. Yoshihara and D. R. Kearns, J. Chem. Phys., **1966**, 45, 1991.
[19] a) A. Gavezzotti, J. Phys. Chem., **1990**, 94, 4319. b) F. H. Allen, C. A. Baalham, J. P. M. Lommerse and P. R. Raithby, Acta Crystallogr., Sect. B: Struct. Sci., **1998**, 54, 320.
[20] a) O. Exner, Dipole Moments in Organic Chemistry, Georg Thieme Publishers, Stuttgart, 1975. b) P. C. Andrews, W. J. Gee, P. C. Junk, H. Krautscheid and J. G. MacLellan, Chem. Commun., **2010**, **46**, 5948. c) S. Lee, A. B. Mallik and D. C. Fredrickson, Cryst. Growth Des., **2004**, 4, 279.
[21] a) J. Tang, S. Zhao, Y. Wei, Z. Quan and C. Hou, Org. Biomol. Chem., **2017**, 15, 1589. b) H. R. Luss, D. L. Smith, Acta Cryst., **1972**, B28, 884.
[22] a) Desiraju, G. R.; Steiner, T. The Weak Hydrogen Bond in Structural Chemistry and Biology; Oxford University Press: New York, 1999. b) J. V. Knichal, W. J. Gee, A. D. Burrows, P. R. Raithby and C. C. Wilson, Cryst. Growth Des., **2015**, 15, 465.
[23] a) H. Ito, M. Muromoto, S. Kurenuma, S. Ishizaka, N. Kitamura, H. Sato and T. Seki, Nat. Comm., **2013**, 4, 2009. b) W. J. Gee, K. Robertson and J. M. Skelton, Eur. J. Inorg. Chem., **2017**, 2628.
[24] a) J. V. Knichal, W. J. Gee, A. D. Burrows, P. R. Raithby, S. J. Teat and C. C. Wilson, Chem. Commun., **2014**, 50, 14436. b) J. V. Knichal, W. J. Gee, C. A. Cameron, J. M. Skelton, K. J. Gagnon, S. J. Teat, C. C. Wilson, P. R. Raithby and A. D. Burrows, Eur. J. Inorg. Chem., **2017**, 1855.
[25] a) I. Agmon, M. Kaftory, J. Appl. Cryst., **1994**, 27, 146. b) S. X. M. Boerrigter, C. J. M. van den Hoogenhof, H. Meekes, P. Bennema, E. Vlieg, J. Phys. Chem. B., **2002**, 106, 4725.
[26] a) M. Prost, L. Canaple, J. Samarut and J. Hasserodt, ChemBioChem, **2014**, 15, 1413. b) K. Wang, W. Shi, J. Jia, S. Chen and H. Ma, Talanta, **2009**, 77, 1795. c) K. Y. Law, R. O. Loutfy, Macromolecules, **1981**, 14, 587. d) J. Mei, N. C. L. Leung, R. T. K. Kwok, J. W. Y. Lam and B. Z. Tang, Chem. Rev., **2015**, 115, 11718.
[27] L. Cui, H. J. Butler, P. L. Martin-Hirsch and F. L. Martin, Anal. Methods, **2016**, 8, 481.
[28] M. J. West and M. J. Went, Forensic Sci. Int., **2008**, 174, 1.
[29] International Fingerprint Research Group (IFRG), J. Forensic Identif., **2014**, 64, 174.

Layout 2:

COMMUNICATION

Grace E. Florence, Katy A. Bruce, Helena J. Shepherd, William J. Gee*

Page No. – Page No.

Metastable 9-fluorenone: Blue-shifted fluorescence, single-crystal-to-single-crystal reactivity, and evaluation as a multi-modal fingermark visualization treatment

The unexpected discovery of two unique emissive forms of 9-fluorenone after using it to treat latent fingerprints has resulted in the characterisation of a new metastable polymorph. This species exhibits single-crystal-to-single-crystal reactivity, blue-shifted fluorescent emission, and potential forensic applications. A structure-property relationship has been posited comparing the ground and metastable forms to promote understanding.